Stabilizing a Blasius boundary layer with Dielectric Barrier Discharge plasma actuation : experimental characterization.

N. Szulga⋆ †, O. Vermeersch⋆, M. Forte⋆ and G. Casalis⋆
...
⋆*ONERA - The French Aerospace Lab*
F-31055, Toulouse, France - natacha.szulga@onera.fr
...
†Corresponding author

Abstract

This paper presents an experimental characterization of Dielectric Barrier Discharge (DBD) plasma actuation on a two dimensional boundary layer around a flat plate using both Laser Doppler Anemometry (LDA) and hot wire probings. The experiments are conducted in a subsonic windtunnel at a freestream velocity $U_\infty = 35$ m/s for a single DBD actuator and several electrical parameters. Hot wire probings are used to quantify the transition delay and mean velocity profiles far enough from the plasma region, while mean velocity profile inside the plasma extent are measured using LDA after the method has been validated from a comparison with hot wire measurements.

Measurements inside the plasma extent allow to quantify the ionic wind contribution to the actuated mean velocity profiles in a case where the transition is delayed by the actuator. A maximal ionic wind of 7 m/s is found to be added 2 mm downstream the actuator for a consumed electrical power of 80 W/m.

1. Introduction

One possible way to reduce aircraft fuel consumption is to delay the boundary layer transition around wings in order to decrease skin friction drag. Stabilizing the boundary layer mean velocity profiles is a possible approach to achieve this aim. Among the possible techniques, plasma actuation turns out to be an interesting solution because of its easy implementation on a surface, the light weight of the actuators and their input energy (electricity) which allows easy control and modulation. In this work, the actuation is performed using a DBD plasma actuator. This type of actuator is constituted of two electrodes stuck on each face of a dielectric material. When an alternative high voltage is applied between the electrodes, the ambient air is ionized. The charged particles drift under the effect of the electric field and create a body force tangential to the wall (the ionic wind), which is used in this case for transition control. Experiments on transition delay have been successfully conducted for two dimensional configurations on a flat plate[1,2] and on a wing profile[3,4] for velocities of 20 and 35 m/s respectively.

A first set of experiments has been made previously on an ONERA-D two dimensional profile.[5] In this case, the transition was induced by Tollmien-Schlichting waves. Mean velocity profiles were measured outside the plasma region and probings along the chord were performed. A maximum transition delay of 6% of chord has been observed for a freestream velocity $U_\infty = 21$ m/s. A first analytic model for the tangential component of the body force field has been developed and integrated in the ONERA in-house boundary layer code 3C3D from these measurements. This model is able to represent the mean velocity profiles in the vicinity of the wall but could not compute the effect of plasma actuation near the upper edge of the boundary layer. As a result, the computed transition delay due to plasma actuation was slightly over predicted.

In this paper, a new set of experiments, conducted on a flat plate and for freestream velocities higher than 30 m/s, are presented. Combined LDA (Laser Doppler Anemometry) and hot wire measurements are performed to assess the effect of DBD plasma actuation on the boundary layer both inside and out of the plasma region. A focus is made on the mean body force effect, also called steady actuation on the delay of a Tollmien-Schlichting (T-S) induced transition. This new set of measurements will allow to improve the existing body force model.

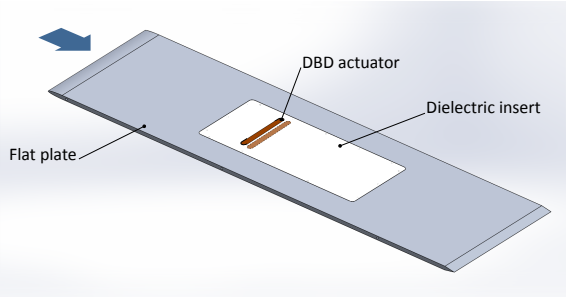

Figure 1: Implementation of the DBD actuator on the flat plate.

2. Experimental set-up

The experiments are conducted in the TRIN 2 subsonic open-return research wind tunnel located at ONERA Toulouse. It features a low turbulence level ($1 \times 10^{-3} \leq Tu \leq 2 \times 10^{-3}$) and a freestream velocity range of $25 \leq U_\infty \leq 50$ m/s, which make it well suited to laminarity and transition studies. The experiments are performed on a flat plate set at a slightly positive angle of attack ($AoA = 0.13°$). The plate is 1.175 mm long and 40 cm wide. It is equipped with a dielectric insert made of PMMA, which allows us to outfit the model with the desired number of actuators between 370 and 820 mm downstream the leading edge. In our case of study, a single DBD actuator is set 100 mm behind the insert upstream edge. The set up of the actuator on the flat plate is presented figure 1. Both electrodes are 21 mm width and their spanwise length is 150 mm. A 2 mm gap separates the electrodes. The actuator is place at $x_{DBD} = 470$ mm from the leading edge.

The air-exposed electrode is connected to a voltage amplifier (Trek, model 30/20A, gain 3000 V/V), while the other is grounded. The input signal has a sinusoidal waveform with orders of magnitude for the amplitude and frequency respectively of 10 kV and 2 kHz. The electric power consumed by a plasma actuator is computed from current and voltage measurements following the relation : $P = \frac{1}{T}\int_0^T V(t) \cdot i(t)\, dt$. A high frequency current transformer (Magnelab, model CT-D0.5, sensibility 0.5 V/A, bandwidth 48 Hz-200 MHz) measures the instantaneous discharge current of the actuator $i(t)$, while $V(t)$ is the instantaneous input voltage given by the monitoring sensor of the amplifier. The average on a sufficiently large number of periods T of $V(t) \cdot i(t)$, computed by a digital oscilloscope (Lecroy wavesurfer 454 bandwidth 500 MHz) gives the mean consumed power P. This value is then divided by the spanwise length of the electrodes to give the consumed power per unit of electrode length $Pa = P/L$ in W/m. The voltage amplitude varies between 9 and 10.8 kV and the input frequency is set at 3 kHz, resulting in a consumed power range between 40 and 80 W/m.

Measurements into the boundary layer are carried out using hot-wire anemometry (Dantec Streamline, 90C10 CTA module, 55P15 probes) and LDA for different configurations with and without control. The laser used for Laser Doppler Anemometry is an Oxxius Laser (wavelength 532 nm, power 300 mW). The emission optics has a 0.46 m focal length. The DISA 55X optic reception is mounted in a forward scattered mode. Seeding is realized using DEHS mineral oil. The measuring volume is about 100 µm in its smaller diameter and 3 mm in its greatest diameter. The optical signal is processed by a digital burst correlator TSI IFA 655. The measurements were conducted for a freestream velocity $U_\infty = 35$ m/s.

3. Baseline flow

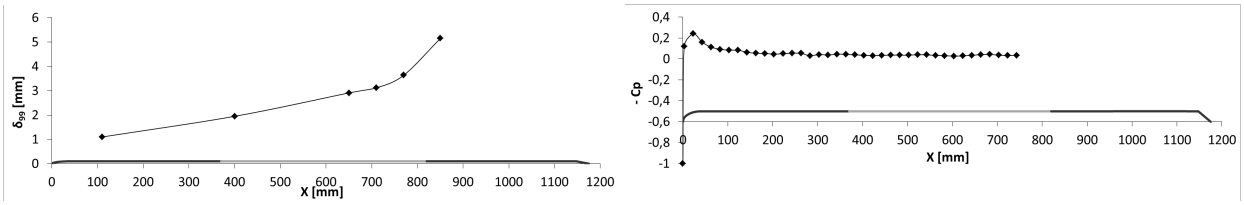

(a) Boundary layer thickness for $U_\infty = 35$ m/s

(b) Measured pressure coefficients

Figure 2: Pressure coefficient and boundary layer thickness evolution along the plate.

As the flat plate is not equipped with pressure taps, the pressure distribution is determined from hot wire measurements. Mean velocity profiles are measured along the flat plate and the boundary layer thickness is assessed for each mean velocity profile. In particular, the boundary layer thickness evolution along the flat plate is given fig. 2a. The pressure coefficient is measured using a hot wire probe placed at the edge of the boundary layer, following the evolution of the boundary layer thickness. The resulting evolution of the pressure coefficient is presented fig. 2b. It features a suction peak followed by a large and weak deceleration which causes the destabilization of the T-S waves. This pressure coefficient distribution is extrapolated in order to allow us to perform boundary layer and stability computations.

The transition location is determined by measuring the hot wire RMS signal along the plate length at a constant height from the wall (z = 1 mm. The tangents of the RMS signal in the laminar and the intermittent phases are then traced (black dotted line on fig. 3). Their intersection gives the transition position. Fig. 3 shows that the natural transition location for U_∞ = 35 m/s is at x_{tr} = 670 mm. This is about 3 cm before the boundary thickens due to a turbulent regime, as seen in fig. 2a. The actuation is performed into the laminar zone.

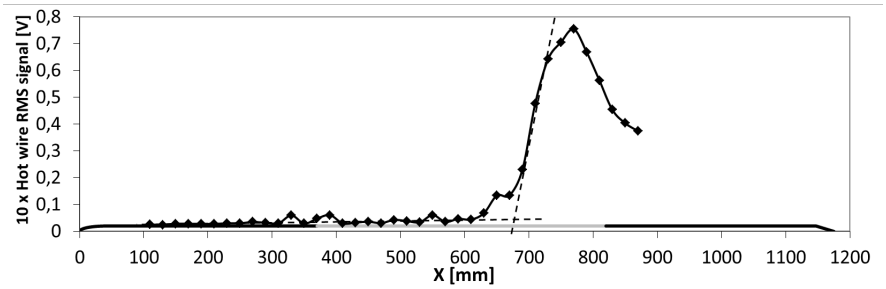

Figure 3: Hot wire RMS signal along the flat plate for U_∞ = 35 m/s.

As the DBD actuator induces a pulsed body force at the same frequency f_p as the input signal,[6] it may excite the corresponding T-S waves and trigger a promoted transition if f_p is not well chosen.[5] For this reason, boundary layer mean velocity profiles have been computed from the experimental pressure distribution using an ONERA in-house boundary layer code (3C3D) and linear stability has then been applied. This results in the N-factor chart of fig. 4 which describes the evolution of the T-S waves amplification along the flat plate. In our case, the turbulence level is $Tu \approx 0.13\%$ which corresponds to a transition N- factor $N_{tr} \approx 7.5$ according to Mack relation ($N_{tr} = -8.43 - 2.4 \cdot \ln(Tu)$).[7] The T-S waves frequency which triggers the transition is f_{tr} = 600 Hz. At the actuator location (x_{DBD} = 470 mm), T-S waves at frequencies below 700 Hz are amplified whereas the others are damped. To avoid any excitation of the T-S waves by the actuation and to focus on a steady actuation, the input signal frequency must be chosen sufficiently higher than the local T-S waves frequencies. Thus, it is set at 3 kHz.

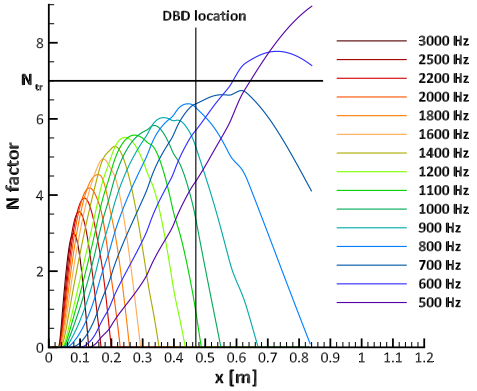

Figure 4: Evolution of T-S waves amplification along the flat plate for U_∞ = 35 m/s.

4. Measurements outside the plasma extent

4.1 Transition measurements

The transition position is determined using the method described in section 3 and illustrated in fig. 3. Fig 5 shows the evolution of a hot wire probe RMS signal along the plate for a boundary layer submitted to DBD plasma actuation at two different consumed powers: P/L = 40 and 80 W/m. The input signal frequency is set at 3 kHz for both cases. For U_∞ = 35 m/s and both consumed power, the actuation results in a transition delay of at least 30 mm. Transition delay could not be measured for a consumed power of 80 W/m. Moreover, the transition delay is greater when the consumed electrical power increases.

In this study, the focus is not set on optimizing the transition delay obtained with the actuator, but to characterize experimentally the influence of steady DBD actuation on a boundary layer flow. Nonetheless, knowing that the transition is delayed confirms that the chosen input signal frequency does not trigger any unwanted unsteady effect.

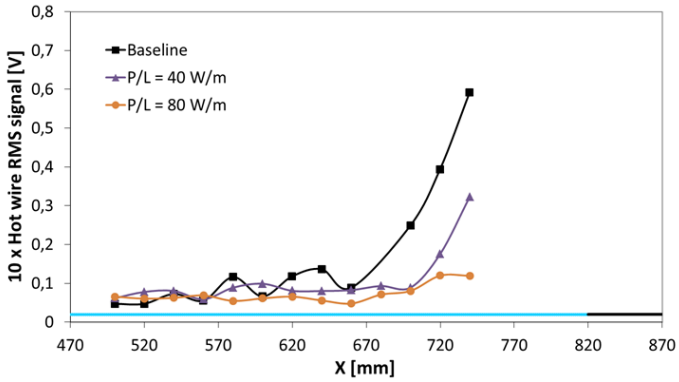

Figure 5: Hot wire RMS signal at a constant height (z = 1 mm) along the plate for U_∞ = 35 m/s and two different actuation cases.

4.2 Mean velocity profiles measurements

Hot wire anemometry is a classical and reliable method to measure mean velocity profiles inside a boundary layer. However, it has to be used far enough from the plasma extent in order to avoid issues due to charges created by the actuator or by the generated electrical field. To ensure that our LDA measurements are well resolved for configurations with and without actuation, mean velocity profiles outside the plasma extent are measured using both LDA and hot wire anemometry at corresponding locations.

Fig. 6 compares the mean velocity profile measured using LDA and hot wire anemometry without actuation at x = 650 mm from the plate leading edge. In the configuration without actuation, the mean velocity profile measured with LDA is in good agreement with the one measured with hot wire.

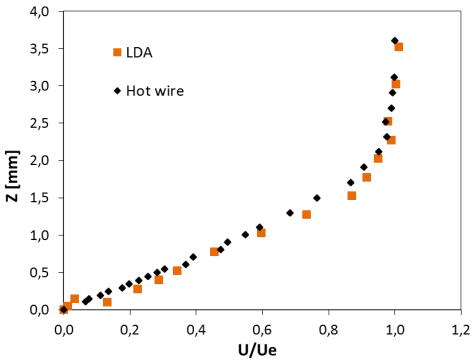

Figure 6: Mean velocity profile measured at x = 650 mm from the leading edge with a hot wire probe and LDA. U_∞ = 35 m/s

Mean velocity profiles measured for two different consumed power (P/L = 40 and 80 W/m) and using both techniques are also compared. Measurements are performed 50 and 100 mm downstream the actuator. The reasulting mean velocity profiles are represented fig. 7 at x_{DBD} + 50 mm and fig. 8 at x_{DBD} + 100 mm. For each case with and without actuation, the measured velocity profiles are compared with the corresponding Blasius one.

Fig. 7a and 8a show mean velocity profiles without actuation measured respectively 50 and 100 mm downstream the actuator using hot wire anemometry. At these locations, the boundary layer is still laminar and the mean velocity profile fits well to the corresponding Blasius mean velocity profile.

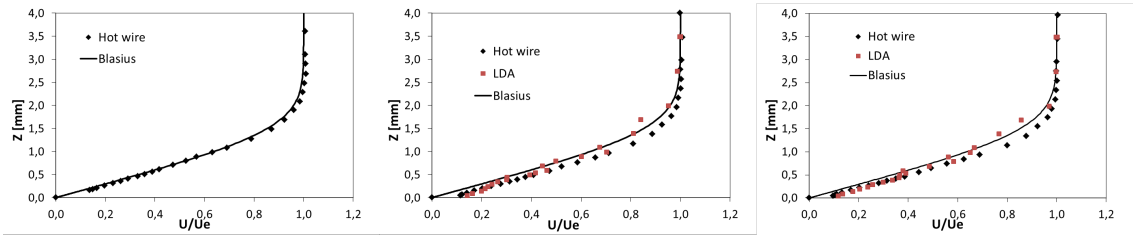

(a) without actuation (b) with actuation, P/L = 40 W/m (c) with actuation, P/L = 80 W/m

Figure 7: Mean velocity profiles measured x_{DBD} + 50 mm compared to a corresponding Blasius velocity profiles for various cases with (b,c) and without (a) actuation.

Fig. 7b and 7c show the effect of DBD actuation at x_{DBD} + 50 mm for P/L = 40 and 80 W/m respectively. At this station and for both actuation cases, the effect of ionic wind is slightly visible over the entire velocity profile. The ionic wind addition results in fuller profiles for both actuation cases. The boundary layer thickness is not affected by the actuation. At this station, we find a great accordance between the velocity profiles measured with LDA and hot wire anemometry.

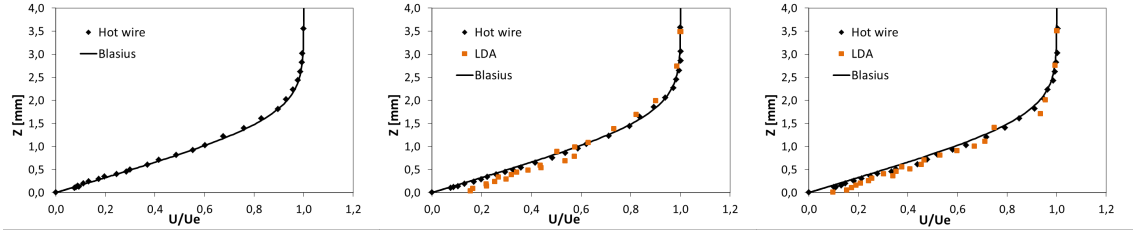

(a) without actuation (b) with actuation,P/L = 40 W/m (c) with actuation,P/L = 80 W/m

Figure 8: Mean velocity profiles measured x_{DBD} + 100 mm compared to a corresponding Blasius velocity profiles for various cases with (b,c) and without (a) actuation.

Fig. 8b and 8c show the effect of DBD actuation at x_{DBD} + 100 mm for P/L = 40 and 80 W/m respectively. The effect of DBD actuation is barely visible on the mean velocity profiles measured using hot wire anemometry. At this station, there is more discrepancy between the LDA and hot wire measurements, especially close to the wall. LDA seems to overestimate the contribution of ionic wind in comparison to the hot wire measurements.

As the boundary layer thickness δ does not change with actuation, a computation of the displacement thickness $\delta_1 = \int_0^\delta \left(1 - \frac{U(z)}{U_e}\right) \mathrm{d}z$ (table 1) is performed to compare the mean velocity profiles "fullness". This computation is made for the mean velocity profiles measured with hot wire anemometry because of their better accuracy.

Table 1: Comparison of the displacement thickness δ_1 (in mm) for the measured mean velocity profiles.

	Baseline	P/L = 40 W/m	P/L = 80 W/m
x_{DBD} + 50 mm	0.8112	0.6974	0.7075
x_{DBD} + 100 mm	0.9436	0.9039	0.8693

The displacement thickness δ_1 decreases for an actuated boundary layer. This value can be seen as the distance of a mean velocity profile to the (non realistic) mean velocity profile where the velocity would be equal to U_e whatever

the distance from the wall. The smaller δ_1 is, the "fuller" the mean velocity profile. In table 1, the contribution of ionic wind which makes the mean velocity profiles fuller, can be seen as far as 100 mm downstream the actuator through this quantity: the more the consumed energy, the "fuller" the velocity profile, and the smaller the displacement thickness.

5. Measurements inside the plasma extent

Hot wire anemometry is limited to measurements outside and sufficiently far from the plasma extent, due to the electrical field which could damage the probe if placed too close to the actuator. To explore the effect of the body force generated by a plasma actuator on the mean velocity profiles inside or close to the plasma extent, LDA is performed.

5.1 Mean velocity profiles

Fig. 9 to 11 show mean velocity profiles measured at several locations inside or close to the plasma extent for different cases with and without actuation. These mean velocity profiles are compared to the corresponding Blasius velocity profile at each location. Each measurement point is colored by the particle rate measured at the same point.

Each actuated mean velocity profile (fig. 9 to 11 b and c) shows a noticeable deformation below $z = 1$ mm from the wall. This change in the mean velocity profiles shape is due to the ionic wind generated by the actuator.

For all the measured velocity profiles, the particle rate decreases as the measurement gets closer to the wall. When comparing velocity profiles with and without actuation, a drop in the particle rate is noticeable when the actuator is powered. Moreover, mean velocity profiles measured for the highest power consumption ($P/L = 80$ W/m) generally show a lower particle rate than the mean velocity profiles measured for $P/L = 41$ W/m. This particle rate decrease when the actuator is powered may be due to the used seeding (DEHS oil), which may not be optimized for measurements with actuation. To improve the measurements quality other kinds of seeding could be tested to find a more adapted solution to our application.

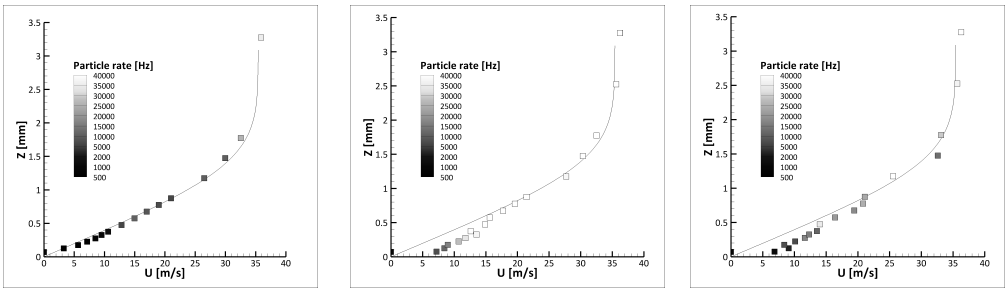

(a) without actuation (b) $P/L = 40$ W/m (c) $P/L = 80$ W/m

Figure 9: Mean velocity profiles measured $x_{DBD} - 2$ mm compared to a corresponding Blasius velocity profile for various cases with and without actuation.

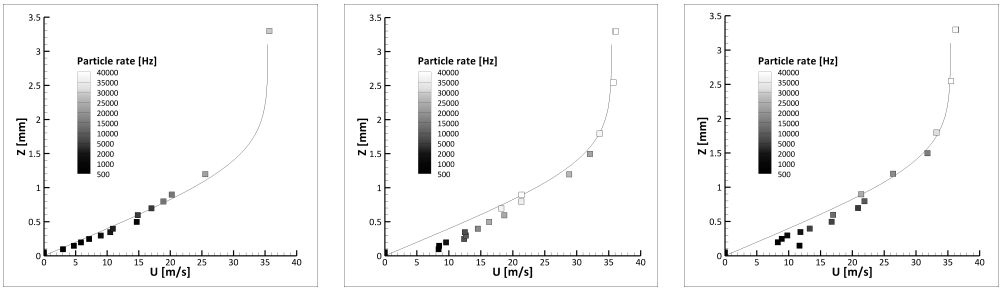

(a) without actuation (b) $P/L = 40$ W/m (c) $P/L = 80$ W/m

Figure 10: Mean velocity profiles measured $x_{DBD} + 2$ mm compared to a corresponding Blasius velocity profile for various cases with and without actuation.

This drop in the particle rate may impact the accuracy of the measured velocity profiles with actuation. Fig. 12 shows the mean velocity profiles measured with and without actuation and with the corresponding errors, for the case at $x_{DBD} + 2$ mm. The error is computed via *bootstrap* theory[8] and is given in m/s and multiplicated by 100 for each measurement point. For all cases, the error increases when measurements are performed closer to the wall.

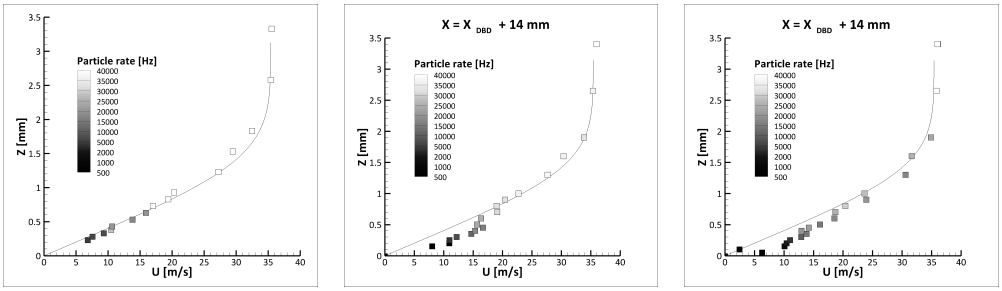

(a) without actuation (b) P/L = 40 W/m (c) P/L = 80 W/m

Figure 11: Mean velocity profiles measured x_{DBD} + 14 mm compared to a corresponding Blasius velocity profile for various cases with and without actuation.

Nonetheless, for the case without actuation (fig. 12a), it is less than 0.1 m/s. This value is obtained at the closest point to the wall, and gives a relative error of 3%. Fig. 12b and 12c show that the error seems to increase when the actuator is powered and that it is generally higher for a higher power consumption. The greatest one is found at the closest point to the wall and for a consumed power of 40 W/m and is less than 0.2 m/s, which represents a relative error of 2% at this station. For every cases with and without actuation, the relative error is reasonable.

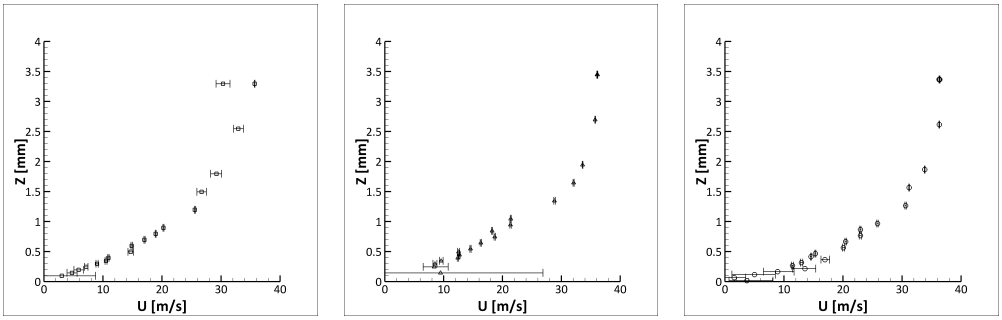

(a) without actuation (b) P/L = 40 W/m (c) P/L = 80 W/m

Figure 12: Mean velocity profiles measured x_{DBD} + 2 mm for various cases with and without actuation, with corresponding error bars. For sake of visibility, error has been multiplication by 100 in these figures.

5.2 Ionic wind contribution in the actuated mean velocity profiles

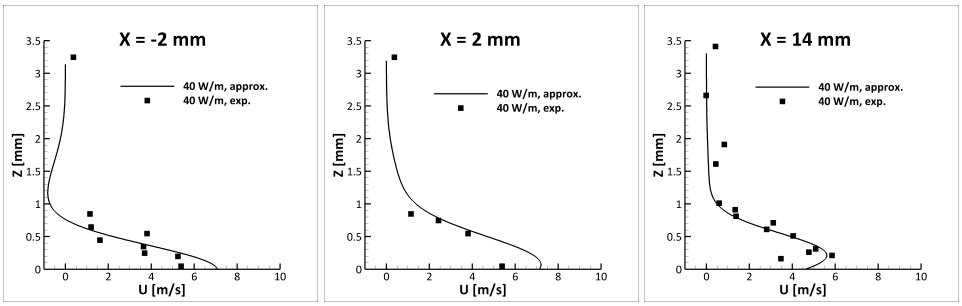

(a) at x_{DBD} − 2 mm (b) at x_{DBD} + 2 mm (c) at x_{DBD} + 14 mm

Figure 13: Added ionic wind at several locations inside and close to the plasma extent for a consumed power P/L = 40 W/m.

The added ionic wind is computed by substracting the baseline one to the actuated ones. Fig. 13 and 14 show the resulting ionic wind contribution evolution inside and close to the plasma extent for the two studied consumed electric powers. Some corresponding experimental points are traced : they are computed by substracting "raw" experimental points at the same height when they existed. For each location, the maximum ionic wind is found at a height $z \leq$

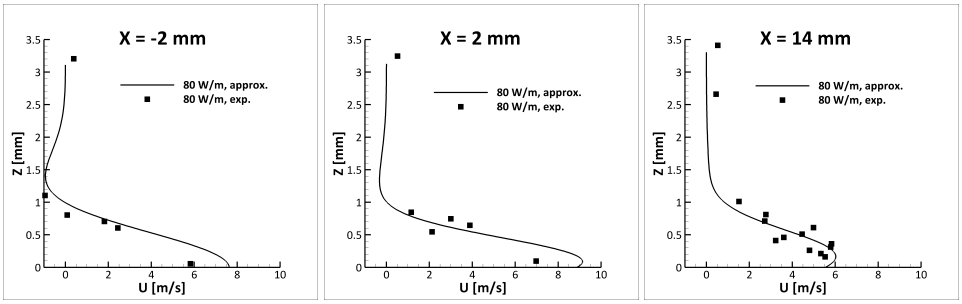

(a) at $x_{DBD} - 2$ mm (b) at $x_{DBD} + 2$ mm (c) at $x_{DBD} + 14$ mm

Figure 14: Added ionic wind at several locations inside and close to the plasma extent for a consumed power $P/L = 80$ W/m.

0.2 mm. Ionic wind diffusion can be seen through the different locations for each control case: the ionic wind maximum shifts away from the wall and the ionic wind profile gets wider when going downstream the actuator. The ionic wind is higher for a consumed power $P/L = 80$ W/m and the maximum found ionic wind addition is found for this power and 2 mm downstream and is around 7 m/s.

Fig. 13a and 14a show that a non-negligible contribution of plasma actuation is brought some millimeters upstream the plasma extent.

6. Conclusions and outlook

In this article, an experimental characterization of DBD plasma actuation on a Blasius boundary layer has been presented. A focus has been made on steady actuation by choosing a suitable input signal frequency: excitation of naturally amplified T-S waves has been avoided. For the presented actuation configurations, a transition delay of at least 30 mm has been obtained, which confirmed the absence of undesired unsteady actuation effects.

Mean velocity profiles measurements have been performed outside and inside the plasma extent. Outside the plasma extent, mean velocity profiles measured with hot wire anemometry and LDA show a great accordance while DBD actuation is performed. Even if 50 and 100 mm downstream the actuator, the ionic wind addition is slightly visible, the boundary layer is still under influence of the actuation, which can be seen as the displacement thickness is greater when the actuator is powered. Inside the plasma extent, mean velocity profiles are measured only with LDA. The plasma actuation effect can be seen below $z = 1$ mm from the wall. The added ionic wind is computed by substracting mean velocity profiles with and without actuation. The maximal measured ionic wind is around 7 m/s for a consumed power $P/L = 80$ W/m 2 mm dowstream the actuator. It has been noticed that the effects of the body force field are visible some millimeters upstream the actuators.

More measurements will be done for other freestream velocities, especially inside the plasma extent. They will allow to enquire about the dependency of the added ionic wind on the freestream velocity. The vertical component of the velocity will also be studied. These sets of measurements will allow to improve an existing empirical body force model, which will be implemented in a boundary layer code. The said model will allow a numerical study of actuation with several DBD actuator will be made to obtained an optimized actuation configuration with several DBD actuators. This configuration will then be experimentally tested.

Acknowledgements

The authors would like to thank Francis Micheli and Estelle Piot for their grateful help with the LDA measurements. Part of this work is supported by the European FP7 Project BUTERFLI (FP7-AAT-2013.8-1-RTD-RUSSIA) program. This work is part of a PhD work which is funded by DGA (Délégation Générale de l'Armement).

References

[1] S. Grundmann and C. Tropea. Experimental transition delay using glow-discharge plasma actuators. *Experiments in Fluids*, 42:653–657, 2007.

[2] R. Joussot, A. Leroy, R. Weber, H. Rabat, S. Loyer, and D. Hong. Plasma morphology and induced airflow characterization of a DBD actuator with serrated electrode. *Journal of Physics D: Applied Physics*, 46(12), March 2013.

[3] A. Séraudie, O. Vermeersch, and D. Arnal. DBD plasma actuator effect on a 2D model laminar boundary layer. Transition delay under ionic wind effect. In *29th AIAA Applied Aerodynamics Conference*, June 2011.

[4] A. Duchmann, B. Simon, C. Tropea, and S. Grundmann. Dielectric barrier discharge plasma actuators for in-flight transition delay. *AIAA Journal*, 52(2):358–367, February 2014.

[5] N. Szulga, O. Vermeersch, M. Forte, and G. Casalis. Experimental and numerical study of boudary layer transition control over an airfoil using a DBD plasma actuator. In *IUTAM_ABCM Symposium on Laminar Turbulent transition*, 2014.

[6] M. Forte, J. Jolibois, J. Pons, E. Moreau, G. Touchard, and M. Cazalens. Optimization of a dielectric barrier discharge actuator by stationary and non-stationary measurements of the induced flow velocity: application to airflow control. *Experiments in Fluids*, 43(6):917–928, November 2007.

[7] L.M. Mack. Transition prediction and linear stability theory. *AGARD Conf. proc. N°224*, 1977.

[8] *An Introduction to the Bootstrap*. Chapman and Hall, 1993.